



Discovery of a series of small molecules as potent histone deacetylase inhibitors

Lei Zhang, Xuejian Wang, Xiaoguang Li & Wenfang Xu

To cite this article: Lei Zhang, Xuejian Wang, Xiaoguang Li & Wenfang Xu (2014) Discovery of a series of small molecules as potent histone deacetylase inhibitors, Journal of Enzyme Inhibition and Medicinal Chemistry, 29:3, 333-337, DOI: [10.3109/14756366.2013.780237](https://doi.org/10.3109/14756366.2013.780237)

To link to this article: <https://doi.org/10.3109/14756366.2013.780237>



Published online: 27 Mar 2013.



Submit your article to this journal [↗](#)



Article views: 728



View related articles [↗](#)



View Crossmark data [↗](#)



Citing articles: 2 View citing articles [↗](#)

ORIGINAL ARTICLE

Discovery of a series of small molecules as potent histone deacetylase inhibitors

Lei Zhang¹, Xuejian Wang², Xiaoguang Li¹, and Wenfang Xu¹

¹Department of Medicinal Chemistry, School of Pharmacy, Shandong University, Jinan, Shandong, China and ²School of Pharmacy and Biology Science, Weifang Medicinal University, Weifang, Shandong, China

Abstract

A series of small molecules were designed and synthesized based on our previous virtual screening approach, which was performed to discover potent histone deacetylase inhibitors (HDACs) with novel structures. The derived compounds were tested by Hela cell nucleus extract for enzyme inhibition assay. Tumor cell growth inhibition assays were performed using a series of tumor cell lines. Molecule **4h** has the best performance among these compounds with enzyme inhibition IC₅₀ of 0.14 μM and tumor cell growth inhibition IC₅₀ of 1.85 (U937), 2.02 (HL60), 2.67 (K562). Docking studies showed that multiple H-bonds and hydrophobic interactions make **4h** binding to the active site of HDAC. **4h** has the advantage of low molecular weight, so a variety of structural modifications can be performed in our further studies.

Introduction

Histone deacetylases (HDACs) are a family of 18 enzymes responsible for the regulation of transcription and other nuclear events by regulating the deacetylation of N-terminal tails of histones. They are subdivided into four classes, class I (HDAC1, 2, 3 and 8), class II (IIa: HDAC4, 5, 7 and 9; IIb: HDAC6 and 10) and class IV (HDAC11) are zinc-dependent enzymes. Class III (known as sirtuins, Sirt1-7) consists of NAD-dependent enzymes^{1–3}. Overexpression and aberrant recruitment of HDACs have a significant role in tumorigenesis^{4–6}.

Histone deacetylase inhibitors (HDACIs) have been proved to have the effects of apoptosis, cell cycle arrest and differentiation^{7–9}. Suberoyl anilide hydroxamic acid (SAHA)¹⁰ and FK228¹¹ have been approved by FDA for treatment of advanced cutaneous T-cell lymphoma (CTCL). Many HDACIs are still under investigation in various stages of clinical trials for treatment of cancer by administration individually or in combination.

In order to discover new scaffold of HDACIs, a virtual screening approach was performed in our previous work¹². A potent small molecule HDAC inhibitor (**02**) was derived as a lead structure. Although **02** has similar enzyme inhibition activity compared with SAHA, it has no activity in the tumor cell growth inhibition assays. Thus, structural modification was performed to discover more potent HDACIs (Figure 1). Hydroxamic acid group was used to bind to zinc ion, sulphonamide and amide groups

Keywords

Docking, histone deacetylase inhibitors, phenylglycine, tumor

History

Received 31 January 2013
Revised 24 February 2013
Accepted 24 February 2013
Published online 25 March 2013

were introduced to the linker to improve H-bond interactions. A series of novel hydroxamic acid-based compounds were synthesized and tested by enzyme inhibition and tumor cell growth inhibition activity assay. A phenylglycine containing structure (**4h**) was discovered to have good performance in these activity assays.

Materials and methods

Chemistry

¹H NMR spectra were recorded on a Bruker DRX spectrometer at 600 MHz, δ in parts per million and J in Hertz, using TMS as an internal standard. High-resolution mass spectra were conducted by Shandong Analysis and Test Center in Ji'nan, China. ESI-MS were determined on an API 4000 spectrometer (AB SCIEX, Framingham, MA). Melting points were determined uncorrected on an electrothermal melting point apparatus. Optical rotation values were measured at room temperature using a modular circular polarimeter 200 operating at λ = 589 nm.

Methyl 4-aminobenzoate hydrochloric acid (**2**)

4-aminobenzoic acid (**1**) (13.7 g, 100 mmol) was dissolved in 100 mL of MeOH, acetyl chloride (23.6 g, 300 mmol) was added under ice bath. The solution was stirred at 75 °C for 5 h. Then, the solvent was evaporated with the desired compound **2** (14.4 g, 77% yield) being recrystallized as white powder by ester. ESI-MS: m/z: 152.1 [M + H]⁺.

(S)-2-((tert-butoxycarbonyl)amino)-2-phenylacetic acid (**h2**)

(S)-2-amino-2-phenylacetic acid (**h1**) (15.1 g, 100 mmol) was dissolved in 200 mL of MeOH/H₂O (3:1), Et₃N (15.1 g, 150 mmol) and (Boc)₂O (32.7 g, 150 mmol) were added in turn.

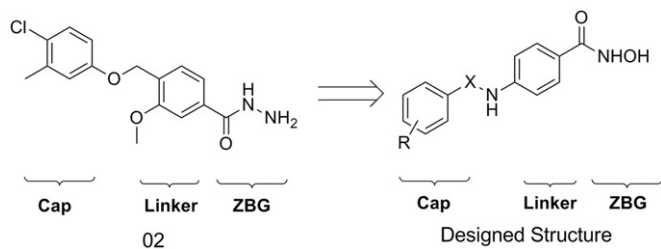


Figure 1. Design of new scaffold from the lead structure.

After stirred at room temperature for 8 h, the solvent was evaporated with the residue being dissolved in saturated citric acid (100 mL). The solution was extracted with EtOAc (3 × 60 mL). The EtOAc solution was washed with saturated brine (3 × 50 mL), dried over MgSO₄, and evaporated under vacuum. The desired compound **h2** (21.6 g, 86% yield) was derived by crystallization in hexane as white powder. ESI-MS: m/z: 252.1 [M + H]⁺.

N-hydroxy-4-(4-nitrophenylsulfonamido)benzamide (**3a**)

To a solution of compound **2** (0.56 g, 3.0 mmol) in THF (50 mL)/H₂O (1.0 mL), NaHCO₃ (1.01 g, 12 mmol) was added. After 10 min, 4-nitrobenzene-1-sulfonyl chloride (0.73 g, 3.3 mmol) was added. The reaction solution was stirred at room temperature for 8 h. Then, the solvent was evaporated with the residue being taken up in EtOAc (50 mL). The EtOAc solution was washed with saturated citric acid (3 × 20 mL), NaHCO₃ (3 × 20 mL) and brine (3 × 20 mL), dried over MgSO₄, and evaporated under vacuum. The desired compound **3a** (0.68 g, 70% yield) was derived by crystallization in EtOAc as white powder. ESI-MS: m/z: 337.1 [M + H]⁺.

The other compounds (**3b–3g**) were prepared in the same procedure as described above.

(*S*)-methyl 4-(2-((*tert*-butoxycarbonyl)amino)-2-phenylacetamido)benzoate (**3h**)

To a solution of **h2** (1.26 g, 5 mmol) in DCM (50 mL), Et₃N (0.55 g, 5.5 mmol) and TBTU (1.8 g, 5.5 mmol) were added in turn. After 20 min, compound **2** (0.94 g, 5 mmol) and Et₃N (0.50 g, 5 mmol) were added. The reaction solution was stirred at room temperature for 8 h. Then, the solvent was evaporated with the residue being taken up in EtOAc (50 mL). The EtOAc solution was washed with saturated citric acid (3 × 20 mL), NaHCO₃ (3 × 20 mL) and brine (3 × 20 mL), dried over MgSO₄, and evaporated under vacuum. The desired compound **3h** (1.44 g, 75% yield) was derived by crystallization in EtOAc as white powder. ESI-MS: m/z: 385.2 [M + H]⁺.

N-hydroxy-4-(4-nitrophenylsulfonamido)benzamide (**4a**)

Compound **3a** (0.5 g, 1.6 mmol) was dissolved in 14 mL of NH₂OK (0.56 g, 24 mmol) methanol solution. After 2 h, the solvent was evaporated under vacuum. The residue was acidified with saturated citric acid, and then extracted with EtOAc (3 × 20 mL). The organic layers were combined, washed with brine (3 × 20 mL) and dried over MgSO₄. The desired compound **4a** (0.33 g, 62% yield) was derived by crystallization in EtOAc as white powder; m.p. = 190–191 °C; ¹H NMR (600 MHz, (CD₃)₂SO) δ 11.08 (s, 1H), 10.63 (s, 1H), 8.95 (s, 1H), 8.38 (d, *J* = 9 Hz, 2H), 8.05 (d, *J* = 8.4 Hz, 2H), 7.65 (d, *J* = 8.4 Hz, 2H), 7.16 (d, *J* = 6 Hz, 2H). HRMS (AP-ESI) m/z calcd for C₁₃H₁₂N₃O₆S [M + H]⁺ = 337.0447, found = 338.0442. Retention time: 2.9 min.

The other compounds (**4b–4h** and **h3**) were prepared in the same procedure as described above.

4-(4-acetamidophenylsulfonamido)-*N*-hydroxybenzamide (**4b**)

Title compound was obtained as an amorphous white solid (0.35 g, 64% yield); m.p. = 214–216 °C; ¹H NMR (600 MHz, (CD₃)₂SO) δ 11.02 (s, 1H), 10.68 (s, 1H), 10.30 (s, 1H), 8.91 (s, 1H), 7.82 (d, *J* = 8.4 Hz, 2H), 7.74 (d, *J* = 10.8 Hz, 2H), 7.71 (d, *J* = 5.4 Hz, 2H), 7.19 (d, *J* = 6 Hz, 2H), 2.06 (s, 3H). HRMS (AP-ESI) m/z calcd for C₁₅H₁₆N₃O₅S [M + H]⁺ = 350.0810, found = 350.0805. Retention time: 2.9 min.

4-(4-chlorophenylsulfonamido)-*N*-hydroxybenzamide (**4c**)

Title compound was obtained as an amorphous white solid (0.32 g, 61% yield); m.p. = 202–204 °C; ¹H NMR (600 MHz, (CD₃)₂SO) δ 11.06 (s, 1H), 10.71 (s, 1H), 8.94 (s, 1H), 7.80 (d, *J* = 8.4 Hz, 2H), 7.65 (d, *J* = 7.2 Hz, 2H), 7.63 (d, *J* = 8.4 Hz, 2H), 7.14 (d, *J* = 9 Hz, 2H). HRMS (AP-ESI) m/z calcd for C₁₃H₁₂ClN₂O₄S [M + H]⁺ = 327.0200, found = 327.0202. Retention time: 2.9 min.

4-(4-fluorophenylsulfonamido)-*N*-hydroxybenzamide (**4d**)

Title compound was obtained as an amorphous white solid (0.28 g, 57% yield); m.p. = 181–183 °C; ¹H NMR (600 MHz, (CD₃)₂SO) δ 11.05 (s, 1H), 10.66 (s, 1H), 8.93 (s, 1H), 7.87 (d, *J* = 8.4 Hz, 2H), 7.63 (d, *J* = 8.4 Hz, 2H), 7.42 (d, *J* = 8.4 Hz, 2H), 7.14 (d, *J* = 8.4 Hz, 2H). HRMS (AP-ESI) m/z calcd for C₁₃H₁₂FN₂O₄S [M + H]⁺ = 311.0502, found = 311.0496. Retention time: 2.9 min.

N-hydroxy-4-(naphthalene-2-sulfonamido)benzamide (**4e**)

Title compound was obtained as an amorphous white solid (0.36 g, 66% yield); m.p. = 237–239 °C; ¹H NMR (600 MHz, (CD₃)₂SO) δ 11.06 (s, 1H), 10.97 (s, 1H), 8.88 (s, 1H), 8.72 (d, *J* = 8.4 Hz, 1H), 8.28 (d, *J* = 7.2 Hz, 1H), 8.23 (d, *J* = 8.4 Hz, 1H), 8.08 (d, *J* = 8.4 Hz, 1H), 7.75 (t, *J* = 7.8 Hz, 1H), 7.68 (d, *J* = 7.2 Hz, 1H), 7.65 (t, *J* = 7.8 Hz, 1H), 7.53 (d, *J* = 8.4 Hz, 2H), 7.08 (d, *J* = 9 Hz, 1H). HRMS (AP-ESI) m/z calcd for C₁₇H₁₅N₂O₄S [M + H]⁺ = 343.0752, found = 343.0746. Retention time: 2.9 min.

4-(2,6-difluorophenylsulfonamido)-*N*-hydroxybenzamide (**4f**)

Title compound was obtained as an amorphous white solid (0.35 g, 63% yield); m.p. = 210–212 °C; ¹H NMR (600 MHz, (CD₃)₂SO) δ 11.24 (s, 1H), 11.05 (s, 1H), 8.94 (s, 1H), 7.20 (d, *J* = 8.4 Hz, 1H), 7.65 (d, *J* = 9 Hz, 2H), 7.30 (d, *J* = 9 Hz, 2H), 7.18 (d, *J* = 8.4 Hz, 2H). HRMS (AP-ESI) m/z calcd for C₁₃H₁₁F₂N₂O₄S [M + H]⁺ = 329.0407, found = 329.0404. Retention time: 2.9 min.

N-hydroxy-4-(4-(trifluoromethyl)phenylsulfonamido)benzamide (**4g**)

Title compound was obtained as an amorphous white solid (0.34 g, 62% yield); m.p. = 249–250 °C; ¹H NMR (600 MHz, (CD₃)₂SO) δ 11.06 (s, 1H), 10.87 (s, 1H), 8.94 (s, 1H), 8.01 (d, *J* = 8.4 Hz, 2H), 7.98 (d, *J* = 9 Hz, 2H), 7.64 (d, *J* = 8.4 Hz, 2H), 7.16 (d, *J* = 9 Hz, 2H). HRMS (AP-ESI) m/z calcd for C₁₄H₁₂F₃N₂O₄S [M + H]⁺ = 361.0470, found = 361.0463. Retention time: 2.9 min.

(*S*)-*tert*-butyl 2-((4-(hydroxycarbonyl)phenyl)amino)-2-oxo-1-phenylethyl carbamate (**4h**)

Title compound was obtained as an amorphous white solid (0.37 g, 63% yield). [α]_D²⁰ = –6.26 (c = 1.0, MeOH); m.p. = 200–202 °C; ¹H NMR (600 MHz, (CD₃)₂SO) δ 11.10 (s, 1H), 10.44

(s, 1H), 8.93 (s, 1H), 7.70 (d, $J=9$ Hz, 2H), 7.63 (d, $J=9$ Hz, 2H), 7.56 (d, $J=8.4$ Hz, 1H), 7.49 (d, $J=7.2$ Hz, 2H), 7.37–7.35 (m, 2H), 7.31 (d, $J=7.2$ Hz, 1H), 5.36 (d, $J=7.2$ Hz, 1H), 1.40 (s, 9H). HRMS (AP-ESI) m/z calcd for $C_{20}H_{23}N_3NaO_5$ $[M+Na]^+$ = 408.1536, found = 408.1529. Retention time: 2.9 min.

(S)-tert-butyl (2-(hydroxyamino)-2-oxo-1-phenylethyl)carbamate (h3)

Title compound was obtained as an amorphous white solid (0.34 g, 61% yield); m.p. = 154–155 °C; $[\alpha]_D^{20} = -6.78$ ($c=1.0$, MeOH). 1H NMR (600 MHz, $(CD_3)_2SO$) δ 10.88 (s, 1H), 8.96 (s, 1H), 7.40 (d, $J=7.8$ Hz, 2H), 7.37 (d, $J=8.4$ Hz, 1H), 7.33 (d, $J=7.2$ Hz, 2H), 7.27 (t, $J=7.2$ Hz, 1H), 5.05 (d, $J=8.4$ Hz, 1H), 1.38 (s, 9H). HRMS (AP-ESI) m/z calcd for $C_{13}H_{18}N_2NaO_4$ $[M+Na]^+$ = 289.1165, found = 289.1158. Retention time: 2.9 min.

(S)-4-(2-amino-2-phenylacetamido)-N-hydroxybenzamide hydrochloride (4hb)

To a solution of compound **4h** (0.38 g, 1 mmol) in EtOAc (10 mL), a solution of EtOAc (15 mL) saturated by dry HCl gas was added. The reaction solution was stirred at room temperature for 5 h. Precipitates appeared and were filtered, with the filter being washed with ether, to give desired compound **4hb** (0.19 g, 68% yield). Title compound was obtained as an amorphous white solid; m.p. = 187–188 °C; $[\alpha]_D^{20} = -6.53$ ($c=1.0$, MeOH). 1H NMR (600 MHz, $(CD_3)_2SO$) δ 11.45 (s, 1H), 10.31 (s, 1H), 8.92–8.91 (m, 3H), 7.73 (d, $J=8.4$ Hz, 2H), 7.70 (d, $J=8.4$ Hz, 2H), 7.69 (d, $J=7.2$ Hz, 2H), 7.46 (d, $J=7.8$ Hz, 2H), 7.43 (t, $J=7.2$ Hz, 1H), 5.33 (d, $J=5.4$ Hz, 1H). HRMS (AP-ESI) m/z calcd for $C_{15}H_{16}N_3O_3$ $[M+H]^+$ = 286.1191, found = 286.1186. Retention time: 2.9 min.

Compound **h4** was prepared in the same procedure as described above.

(S)-2-amino-N-hydroxy-2-phenylacetamide hydrochloride (h4)

Title compound was obtained as an amorphous white solid (0.21 g, 70% yield); m.p. = 209–210 °C; $[\alpha]_D^{20} = -7.21$ ($c=1.0$, MeOH). 1H NMR (600 MHz, $(CD_3)_2SO$) δ 11.10 (s, 1H), 9.30 (s, 1H), 8.87 (s, 3H), 7.56 (d, $J=6.6$ Hz, 2H), 7.45 (d, $J=7.2$ Hz, 2H), 7.43–7.41 (m, 5H), 4.85 (s, 1H). HRMS (AP-ESI) m/z calcd for $C_8H_{11}N_2O_2$ $[M+H]^+$ = 167.0820, found = 167.0810. Retention time: 2.9 min.

Enzyme inhibition assay

The HDAC enzyme was extracted from Hela cells. Boc-Lys (acetyl)-AMC was used as the substrate of HDAC. SAHA which is the HDAC inhibitor on market was used as a positive control. The compounds were diluted to six concentrations (25, 5, 1, 0.2, 0.04 and 0.008 μ M/L) to investigate their ability of inhibiting HDAC activity.

Tumor cell inhibition assay

HCT116, K562, MDA-MB-231, ES-2, U937, HL60, MCF7 and PC3 cells were used in the cell proliferation assays. A total of 5000 cells were seeded into each well of 96-well plates which were incubated at 37 °C, 5% CO_2 for overnight. Then cells (HCT116, K562, MDA-MB-231, ES-2) were treated with 5 μ M of all these molecules. In order to calculate the IC_{50} values, cells (U937, HCT116, K562, HL60, MCF7 and PC3) were treated with compound **4h** and SAHA at final concentrations ranging from 0.25 to 20 μ M. After 48 h of incubation, 0.5% MTT

(Amresco, Solon, OH) solution was added to each well. Then a further 4 h of incubation was performed. After that the culture medium was removed, and 200 μ L of DMSO was added to dissolve the formazan. After mixing for 5 min, optical density values were detected at 570 nm on a microplate reader (Thermo Fisher Scientific, Waltham, MA).

Molecular docking

The molecular docking process was performed using Glide (www.schrodinger.com). Crystal structure of HDAC2 (PDB Entry: 3MAX) was selected as a receptor in the docking study. Structural modifications were performed to make the protein suitable for docking. The water molecules and the ligand crystallized in the protein structure were removed. OPLS 2005 force field was assigned to the refined structure. The ligands used in the docking approach were sketched by maestro and prepared by LigPrep (www.schrodinger.com). The active site was defined as a cubic box containing residues around Zn ion at a distance of 20 Å. Extra precision was applied in the docking process, other parameters were set as default.

Results and discussion

Chemistry

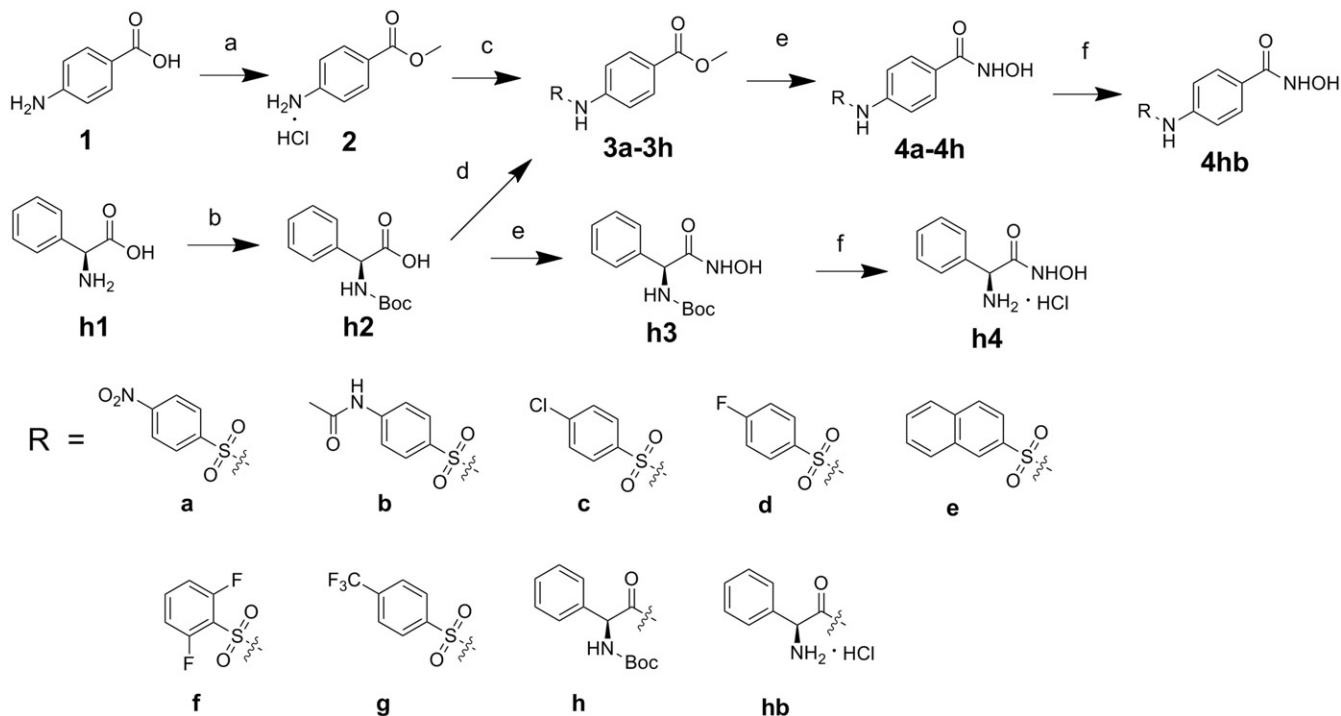
The target compounds were synthesized following the route shown in Scheme 1. The starting material 4-aminobenzoic acid was converted to be compound **2** by esterification. The key intermediates (**3a–3g**) were generated by nucleophilic substitution of compound **2** with corresponding sulfonyl chloride^{13–18}. L-phenylglycine was protected by Boc, followed by coupling with compound **2** to yield **3h**. Compounds **4a–4h** were derived by treating the corresponding intermediates (**3a–3h**) with NH_2OK in methanol¹⁹. Compound **4hb** was derived by deprotection of the amino group of **4h**. Compounds **h3** and **h4** were prepared via the same route as **4hb**.

Activity assay

The derived compounds were assayed by Hela cell nucleus extract using SAHA as a positive control (Table 1). Molecule **4h** has the best performance in the enzyme inhibition assay. Among compounds **4a–4g**, **4e** has the best enzyme inhibition activity. The result means bulky R groups are beneficial for these molecules binding to HDACs. Protection of the amino group by Boc group in the phenylglycine improved the activity, which was proved by comparing the IC_{50} values between **4h** (0.14 μ M) and **4hb** (0.18 μ M), **h3** (1.60 μ M) and **h4** (3.79 μ M). The results indicate that substituent in the amino group improves the interaction between the ligands and the receptor. Molecules **h3** and **h4** were subsequently synthesized to find out if the phenylglycine structure has enzyme inhibition activity without a linker. The results suggest that removal of the linker results in the reduction of the activity.

The results of the tumor cell growth inhibition assay have correlation with the results of the enzyme inhibition assay (Table 1). K562 cells are more sensitive to these molecules than other cells. In these assays, **4h** is also the most potent inhibitor. Deprotection of the amino group in the phenylglycine and removal of the linker have significant influence on the inhibitory activity.

The IC_{50} values of **4h** in inhibition of U937, HCT116, K562, HL60, MCF7 and PC3 cell growth were derived compared with SAHA (Table 2). The results showed that **4h** could efficiently inhibit the growth of these cell lines. In inhibition, the growth of K562, HL60 and PC3 cells, **4h** even has similar performance with SAHA. Our results also indicate that **4h** can selectively inhibit the growth lymphoma cells and hematological tumor cells.



Scheme 1. Reagents and conditions: (a) CH_3COCl , CH_3OH ; (b) $(\text{Boc})_2\text{O}$, Et_3N , $\text{MeOH}/\text{H}_2\text{O}$; (c) RSO_2Cl , NaHCO_3 , $\text{THF}/\text{H}_2\text{O}$; (d) TBTU, Et_3N , THF; (e) NH_2OK , MeOH ; (f) EtOAc , HCl .

Table 1. The inhibitory activities of derived molecules.*

Compounds	IC_{50}^\ddagger (μM)	HCT116 (inhib%) ‡	K562 (inhib%)	MDA-MB-231 (inhib%)	ES-2 (inhib%)
4a	0.28	3.36	24.59	24.35	1.48
4b	0.74	3.77	22.75	11.40	5.07
4c	0.33	17.49	50.79	28.55	23.49
4d	1.42	20.51	55.63	21.98	13.33
4e	0.23	8.12	56.77	36.99	44.16
4f	1.05	8.31	8.22	3.05	16.73
4g	2.11	3.04	27.86	3.71	13.59
4h	0.14	22.32	57.79	35.98	50.01
4hb	0.18	8.66	50.44	9.73	32.71
h3	2.60	7.33	41.35	8.21	12.33
h4	3.79	4.65	34.88	5.06	9.55
SAHA	0.17	35.11	56.84	44.68	47.19

*The method for *in vitro* activity assay has been described in our previous work²⁰.

‡ Each value is the mean of at least three experiments (all SDs are within 10% of the mean).

‡ The activity was described as inhibition%, the concentration of the molecules is 5 μM .

Table 2. The tumor cell growth inhibitory activities of 4h compared with SAHA.*

Compounds	U937	HCT116	K562	HL60	MCF7	PC3
4h	1.85	12.12	2.67	2.02	12.70	4.93
SAHA	0.99	4.21	2.99	1.86	5.09	6.33

*Each value is the mean of at least three experiments (all SDs are within 10% of the mean).

Binding pattern analysis

Docking study was performed to simulate the binding pattern between 4h and HDAC. In order to seek evidence for the difference of the activity between 4h and 4hb, 4hb was also docked to the active site of HDAC2. The docking result shows

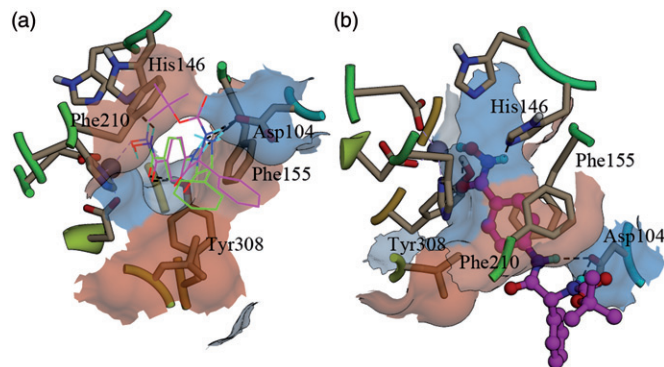


Figure 2. Binding patterns of 4h and 4hb in the active site of HDAC2: (a) 4h and 4hb were shown using the wire model, the residues were displayed as sticks; carbon atoms of 4h were colored magenta, carbon atoms of 4hb were colored green, the gray ball is zinc ion, the H-bonds were represented as dash lines (in black–white mode, 4h is the structure containing Boc group); (b) 4h was shown using the ball–stick model.

that 4hb has similar binding pattern with 4h (Figure 2a). The hydroxamic acid groups of both molecules play a significant role in binding the ligands to the receptor by chelating to the zinc ion and forming H-bond interactions with residues around zinc ion (Figure 2b). The ketonic oxygen of the hydroxamic acid group has H-bond interaction with the phenolic hydroxyl group of Tyr308. Nevertheless, the amino group binds to the NE2 of His146 by forming H-bond interactions. The hydroxyl group of Asp104 has H-bond binding with the other two amino groups, which also make important contributions to the binding. The benzene ring of the linker has π – π stacking interactions with the phenyl groups of Phe155 and Phe210, which improves the binding of these two molecules to the active site of HDAC.

Conclusion

In order to develop potent HDAC inhibitors with efficient tumor cell inhibitory activities, a series of small molecules were

synthesized based on our previous virtual screening results. The enzyme inhibition assay and tumor cell growth inhibition assay results show that **4h** is the most potent HDAC inhibitor. Moreover, **4h** also has good performance in inhibiting the growth of a series of tumor cell lines compared with SAHA. An important finding is introduction of bulky group to the amino group of the phenylglycine part that can obviously improve the inhibitory activity. Our work emphasizes the prospect and necessity of development HDAC inhibitors with various substituent groups in the amino group of phenylglycine in our further work.

Declaration of interest

The authors report no conflicts of interest. The authors alone are responsible for the content and writing of this article.

This work was supported by National Nature Science Foundation of China (Grant No. 90713041), National High Technology Research and Development Program of China (Grant No. 2007AA02Z314 and 2009ZX09103-118) and Graduate Innovation Foundation of Shandong University (GIFSDU) (No. yyx10020).

References

- Bernstein BE, Tong JK, Schreiber SL. Genomewide studies of histone deacetylase function in yeast. *P Natl Acad Sci USA* 2000;97:13708–13.
- De Ruijter AJM, Van Gennip AH, Caron HN, et al. Histone deacetylases (HDACs): characterization of the classical HDAC family. *Biochem J* 2003;370:737–49.
- Foglietti C, Filocamo G, Cundari E, et al. Dissecting the biological functions of *Drosophila histone* deacetylases by RNA interference and transcriptional profiling. *J Biol Chem* 2006;281:17968–76.
- Bode AM, Dong ZG. Post-translational modification of p53 in tumorigenesis. *Nat Rev Cancer* 2004;4:793–805.
- Chen LF, Greene WC. Shaping the nuclear action of NF-kappa B. *Nat Rev Mol Cell Bio* 2004;5:392–401.
- Kovacs JJ, Murphy PJM, Gaillard S, et al. HDAC6 regulates Hsp90 acetylation and chaperone-dependent activation of glucocorticoid receptor. *Mol Cell* 2005;18:601–7.
- Marks PA, Rifkind RA, Richon VM, et al. Histone deacetylases and cancer: causes and therapies. *Nat Rev Cancer* 2001;1:194–202.
- Johnstone RW. Histone-deacetylase inhibitors: novel drugs for the treatment of cancer. *Nat Rev Drug Discov* 2002;1:287–99.
- Insinga A, Monestiroli S, Ronzoni S, et al. Inhibitors of histone deacetylases induce tumor-selective apoptosis through activation of the death receptor pathway. *Nat Med* 2005;11:233.
- Richon VM, Emiliani S, Verdin E, et al. A class of hybrid polar inducers of transformed cell differentiation inhibits histone deacetylases. *P Natl Acad Sci USA* 1998;95:3003–7.
- Ueda H, Nakajima H, Hori Y, et al. Fr901228, a novel antitumor bicyclic depsipeptide produced by chromobacterium-violaceum no-968.1. Taxonomy, fermentation, isolation, physicochemical and biological properties, and antitumor-activity. *J Antibiot* 1994;47:301–10.
- Zhang L, Li MY, Feng JH, et al. Discovery of a novel histone deacetylase 8 inhibitor by virtual screening. *Med Chem Res* 2012;21:152–6.
- D'Ambrosio K, Smaine F-Z, Carta F, et al. Development of potent carbonic anhydrase inhibitors incorporating both sulfonamide and sulfamide groups. *J Med Chem* 2012;55:6776–83.
- Akdemir A, Vullo D, Luca VD, et al. The extremo-alpha-carbonic anhydrase (CA) from *Sulfurihydrogenibium azorense*, the fastest CA known, is highly activated by amino acids and amines. *Bioorg Med Chem Lett* 2013;23:1087–90.
- Allouche F, Chabchoub F, Carta F, Supuran CT. Synthesis of aminocyanopyrazoles via a multi-component reaction and anti-carbonic anhydrase inhibitory activity of their sulfamide derivatives against cytosolic and transmembrane isoforms. *J Enzym Inhib Med Chem* 2013;28:343–9.
- Alp C, Maresca A, Alp NA, et al. Secondary/tertiary benzenesulfonamides with inhibitory action against the cytosolic human carbonic anhydrase isoforms I and II. *J Enzym Inhib Med Chem* 2013;28:294–8.
- Maresca A, Scozzafava A, Vullo D, Supuran CT. Dihalogenated sulfanilamides and benzolamides are effective inhibitors of the three beta-class carbonic anhydrases from *Mycobacterium tuberculosis*. *J Enzym Inhib Med Chem* 2013;28:384–7.
- Supuran CT, Maresca A, Gregan F, Remko M. Three new aromatic sulfonamide inhibitors of carbonic anhydrases I, II, IV and XII. *J Enzym Inhib Med Chem* 2013;28:289–93.
- Su L, Cao J, Jia Y, et al. Development of synthetic aminopeptidase N/CD13 inhibitors to overcome cancer metastasis and angiogenesis. *ACS Med Chem Lett* 2012;3:959–64.
- Zhang YJ, Feng JH, Liu CX, et al. Design, synthesis and preliminary activity assay of 1,2,3,4-tetrahydroisoquinoline-3-carboxylic acid derivatives as novel histone deacetylases (HDACs) inhibitors. *Bioorg Med Chem* 2010;18:1761–72.